J Mol Model (2011) 17:1457–1465
DOI 10.1007/s00894-010-0840-3

ORIGINAL PAPER

Molecular dynamics study of solvation effect on diffusivity changes of DNA fragments

Kentaro Doi · Takamasa Uemura · Satoyuki Kawano

Received: 13 April 2010 / Accepted: 30 August 2010 / Published online: 19 September 2010

Abstract DNA sequence analyzing and base pair separation techniques have attracted much attention, such as denaturing gradient gel electrophoresis, temperature gradient gel electrophoresis, and capillary electrophoresis. However, details of sequence separation mechanisms in electrophoresis are not clarified enough. Understanding and controlling flow characteristics of DNA are important not only for fundamental research but also for further developments of bio-nano technologies. In the present study, we theoretically discuss the relationship between diffusivity and hydrated structures of DNA fragments in water solvent using molecular dynamics methods. In particular, influence of base pair substitutions on the diffusivity is investigated, focusing on an adenine-thymine (AT) rich B–DNA decamer 5'-dCGTATATATA-3'. Consequently, it is found that water molecules that concentrate on dissociated base pairs form hydrated structures and change the diffusivity of DNA decamers. The diffusion coefficients are affected by the substitution of GC for AT because of the different manner of interactions between the base molecules and water solvent. This result predicts a possibility of base pair separation according to differences in the diffusivity.

Keywords Bio-nano technology · Diffusivity · DNA · Hydrated structure · Molecular dynamics · Single nucleotide polymorphism

K. Doi (✉) · T. Uemura · S. Kawano
Department of Mechanical Science and Bioengineering,
Graduate School of Engineering Scienece, Osaka University,
Osaka 560-8531, Japan
e-mail: doi@me.es.osaka-u.ac.jp

Introduction

Recently, effective techniques for DNA sequence separation have been developed. The denaturing gradient gel electrophoresis (DGGE) [1, 2] and the temperature gradient gel electrophoresis (TGGE) [3–5] are familiar methods to investigate the characteristics of DNA sequences. Using these techniques, single nucleotide polymorphisms (SNPs) can be detected as a result of differences in their displacements under applied electric fields. It is considered that meaningful differences are obtained from the molecular sieving effect of denatured base sequences. Further details about SNP analyses are summarized in several review articles [6, 7]. In addition, measurements using capillary electrophoresis (CE) are also known to be effective for separating the size of DNA fragments [8–11]. High accuracy to measure the fragment sizes can be achieved using CE.

Furthermore, novel techniques for DNA sequence separations have been developed focusing on nanoscale flow dynamics of DNAs [12–16]. In nanoscale spaces, atomic interactions between molecules and surroundings seem to dominate the phenomena. Influences of surrounding surface conditions on molecular fluidity were experimentally observed [14, 16]. Meanwhile, a novel technique to detect base sequences were suggested by the use of nanoscale electrodes implemented in nano channels [15]. These measurements were succeeded by controlling electronic properties of DNAs [17]. Possibilities of single nucleotide detection were also discussed from theoretical aspects [18–21].

As mentioned above, the characteristics of DNA were well understood based on the hydrodynamics. However, the detailed mechanism of molecular sieving in terms of the molecular mechanics and atomic interactions has not been clarified enough yet. In this study, we focus on the nature of molecular interactions between DNA fragments and solvent

media expected to cause detection of SNPs. Our interest is in the process of sequence separation resulted from electrostatic and van der Waals (VDW) interactions between the solute and solvent molecules. Using molecular dynamics (MD) computations [22–24], it is simulated whether the diffusivity of DNA fragments is actually influenced by solvent molecules that form hydrogen bonds with dissociated base molecules. Instead of gel media that has complicated porous structures, water solvent is adopted in order to analyze the influence of atomic interactions on the diffusivity. Hydration effects on DNAs and the molecular structures were well investigated in terms of experiments and computations [25–32]. On the other hand, hydrated structures of DNA sequences, in which complementary base pairs are completely bonded, have been investigated because dynamics of water molecules near DNA surfaces are considered to affect an interesting transition: B–DNA ↔ A–DNA [34–36]. However, the diffusivity change of DNA fragments in which complementary base pairs are partly dissociated has not been discussed enough. In previous studies, we developed coarse-grained DNA models [18, 33] and investigated their flow dynamics in solvent media. It was concluded that interactions between base molecules, phosphate groups, and solvent molecules play an important role in the flow dynamics of DNA and that their atomic interactions should be treated in detail. Therefore, the present study is expected to provide suggestive results for further developments.

As a result of the present computations, it is found that base pair cleavages in DNA fragments clearly influence the diffusivity. Hydrated structures particularly increase around N atoms that become bare with base pair cleavages. The difference of molecular conformations in adenine-thymine (AT) and guanine-cytosine (GC) base pairs appears to influence the hydrated structures. The behavior of DNA fragments is perturbed by the hydrogen bonds with solvent molecules. It is indicated that the mutations of single base pairs affect the diffusivity changes of DNA fragments. The present results partly explain the molecular sieving effect that is caused by interactions between denatured DNA fragments and surrounding solvent molecules.

Models and computational methods

DNA decamer models

Figure 1 shows illustrations of complementary AT and GC base pairs that form double and triple hydrogen bonds, respectively. The hydrogen bonds dominate the bond strength or melting temperature of base pair sequences [37]. In the present study, N and O atoms, such as N1(A), O2(T), O4(T), N3(C), O2(C), and O6(G) marked with open circles in Fig. 1, are focused because these atoms turn to be bare and interact strongly with solvent molecules as the DNA sequences are denatured. For comparison, hydrated structures around O2(T) that does not form hydrogen bonds with its complementary pair are additionally investigated. In some cases, protons may be exchanged between the complementary base pairs. In this study, however, the proton transfer mechanisms between complementary base pairs are not treated and they are discussed elsewhere [38]. As shown in Fig. 2, DNA fragments composed of 10 base pairs (10 bp) are prepared for the present MD computations. These models are constructed based on Watson-Crick B-form DNA (B–DNA). The sequence of 5'-dCGTATA-TATA-3' is located in water solvent. Base molecules are sequentially assigned as C1 to A10 for the convenience of discussion. Alignments in the opposite strand are sequentially represented as G11 to T20. Figure 2a shows one of the models, hereafter referred to as model **a**, in which each hydrogen bond between complementary base pairs is connected completely. Another one shown in Fig. 2b is referred to as model **b** in which 8 AT base pairs are sufficiently dissociated. Using these models, the diffusivity of DNA fragments is investigated focusing on the hydrated structures formed around dissociated sites. The GC pairs

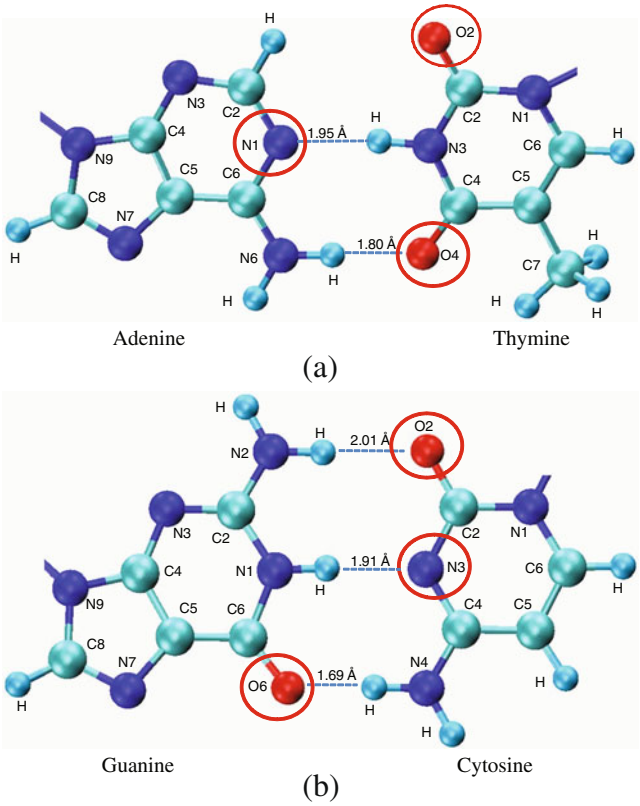

Fig. 1 Schematic illustrations of complementary (**a**) AT and (**b**) GC base pairs. Base atoms N1(A), O2(T), O4(T), N3(C), O2(C), and O6(G) are focused, which form hydrogen bonds with solvent molecules due to base pair cleavages

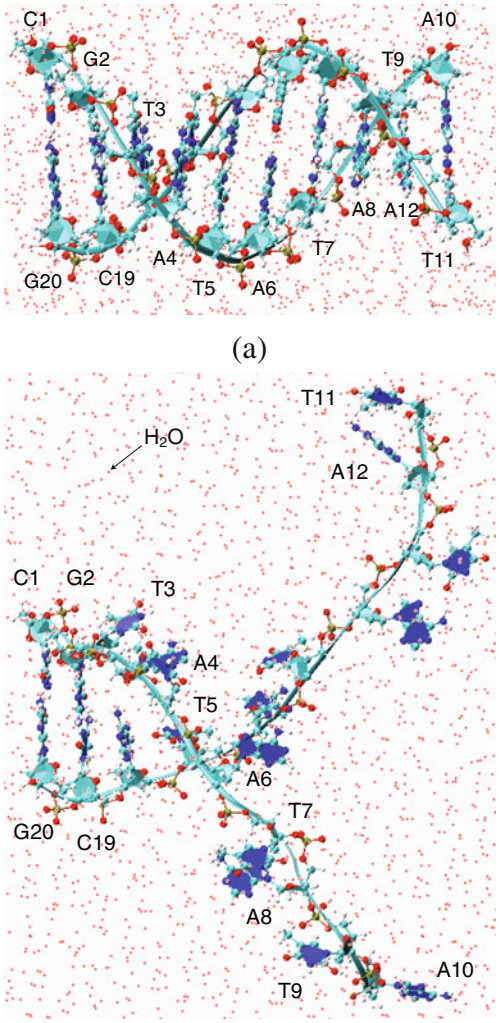

Fig. 2 Schematic illustrations of (**a**) B–DNA and (**b**) denatured DNA decamers in water solvent

placed at the edge have a role of GC clamp. In addition, other sequences in which AT pairs are partly replaced by a GC pair are also prepared to investigate their effects on the diffusivity. Some kinds of mutations are prepared, in which A4T17, A6T15, A8T13, and A10T11 are replaced by G4C17, G6C15, G8C13, and G10C11, respectively. These models are respectively referred to as models **c**, **d**, **e**, and **f** and their detailed sequences are summarized in Table 1. Water molecules in the solvent medium are presented by SPC/E model [39] that is known to be in good agreement with experimental measurements on pure water. Additionally, covalent bonds caused by H atoms except for hydrogen bonds are fixed using SHAKE method [40]. Our main purpose is to discuss hydrogen bonds concerned with water molecules attracted to dissociated base pairs and is not to investigate the covalent bond breakings. Therefore, using SHAKE method, the computational labor is expected to be reduced efficiently. Counter cations of Na^+ are contained in order to neutralize negative charges on the backbones of DNA. The system is in the periodic boundary condition of truncated octahedron and is so large that interactions between DNA fragments in each image cell are negligible. The amount of water molecules filled in a cell is between 13998 and 14001, that is determined from the density of pure water.

MD computations for DNA decamers

In a previous step of MD sampling, structural equilibration and temperature control are carried out. In the case of **b**, **c**, **d**, **e**, and **f**, the denatured structures of DNA fragments are developed by hand on the graphical user interface. Their molecular structures are optimized in water solvent and several metastable structures that are employed as the initial conditions of MD computations are found. Figure 2b shows a metastable denatured structure of the case **b**. Molecular structures are equilibrated in isothermal and isovolumetric conditions. The initial momenta of each molecule are set according to the Maxwell distribution. The Langevin thermostat is adopted to maintain the constant temperature of 300 K. In each case, the systems are relaxed in the isothermal and isovolumetric condition at first 10 ps. Continuously, the molecular distributions are equilibrated under the constant pressure of 0.1 MPa for 100 ps. Furthermore, the systems are relaxed in the canonical ensemble for 10 ps . After these equilibration processes, MD samplings are carried out for 250 ps. A time step in the MD samplings is suitably chosen at 1.0 fs that progresses the time evolutions stably maintaining the conservation laws. VDW and Coulomb interactions are taken into account up to 10 Å and 30 Å, respectively, those distances are long enough to ignore each effect from the farther side. In the equilibrium conditions, MD samplings are performed under the microcanonical ensemble in which each system is confirmed to move near the equilibrium states. The temperature is fluctuated near 300 K. In these MD procedures, the force field of FF03 [41] is employed for

Table 1 10 bp DNA sequences for MD computations

Model	Sequence	Condition
a	5'-dCGTATATATA-3'	B–DNA
b	5'-dCGTATATATA-3'	Denatured
c	5'-dCGTGTATATA-3'	Denatured
d	5'-dCGTATGTATA-3'	Denatured
e	5'-dCGTATATGTA-3'	Denatured
f	5'-dCGTATATATG-3'	Denatured

atomic interactions and the computations are performed using a computational code Amber 10 [42].

In order to discuss the effect of hydrated structures on the diffusivity, water molecules that contribute to the hydration are counted by the radial distribution function:

$$g(r) = \frac{n(r)}{4\pi r^2 \rho \Delta r}, \tag{2.1}$$

where the number of water molecules $n(r)$ within a spherical shell between $r - \Delta r/2$ and $r + \Delta r/2$ is divided by the number density of pure water ρ, which is presented as 0.0333 $Å^{-3}$ at 300 K. The distribution function is calculated with the interval of Δx=0.1 Å.

Mean square displacements are evaluated from the results of MD samplings and the molecular diffusivity is calculated from the Einstein relation [43]:

$$D = \lim_{t\to\infty} \frac{1}{6t} \left\langle |\mathbf{R}(t) - \mathbf{R}(0)|^2 \right\rangle, \tag{2.2}$$

where, $\mathbf{R}(t)$ is a position vector of the center of mass at time t. The diffusion coefficient of Eq. 2.2 is evaluated from the average of several trials for each 250 ps sampling. In the present study, in order to cover the brief samplings of each trial in the microcanonical ensemble, mean square displacements are evaluated from the average of 6 time trials. Based on this procedure, linearity of mean square displacements is well maintained.

Results and discussion

Effects of base pair dissociation and hydrated structures on diffusivity

Figure 3 shows the radial distribution functions of water molecules around B–DNA (**a**) and denatured DNA (**b**) decamers, where each distribution presents averaged amounts of water molecules around 8 AT base pairs. Differences in the distributions appear remarkably very near the DNAs. The concentrations of water molecules around N1(A) and O4(T) are particularly featured because they lose hydrogen bonds between complementary base pairs and are activated by the base pair cleavages. In Fig. 3a, the radial distribution function and the number of water molecules around N1(A) in **a** and **b** are presented. In this case, apparent differences are obtained between the B–DNA and the denatured DNA. The distribution of water molecules is very dilute around N1(A) in **a** and the density turns to be lower than that of pure water. Meanwhile, the distribution drastically increases due to the base pair cleavages. The high concentration of water molecules, which is denser than that of pure water, appears at the distance of near 2.0 Å. This is because water molecules are

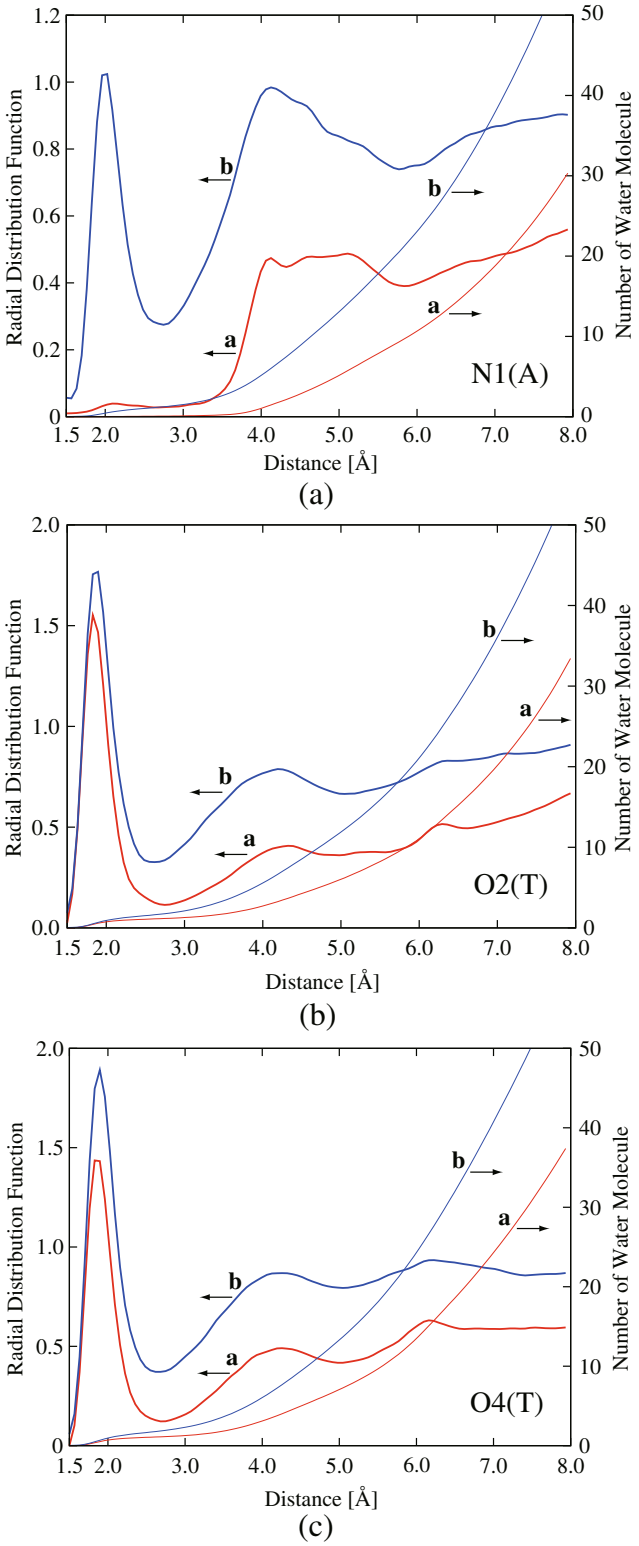

Fig. 3 Radial distribution function and number of water molecules around (**a**) N1(A), (**b**) O2(T), and (**c**) O4(T). In each case, interactions between base atoms and water molecules become strong and water molecules concentrate on these base atoms due to base pair cleavages

Table 2 Amount of water molecules within 2.5 and 3.4 Å around N1(A), O2(T) and O4(T). Standard deviations are in parentheses

	N1(A)		O2(T)		O4(T)	
	2.5 Å	3.4 Å	2.5 Å	3.4 Å	2.5 Å	3.4 Å
a	0.1 (0.1)	0.2 (0.3)	1.1 (0.1)	1.6 (0.2)	1.0 (0.1)	1.7 (0.3)
b	1.0 (0.1)	2.3 (0.4)	1.5 (0.1)	3.1 (0.3)	1.7 (0.1)	3.3 (0.3)

attracted to the dissociated N1(A) and hydrogen bonds are formed between them. In addition, the difference in the amount of water molecules is observable over a long distance. Figure 3b shows the distributions around O2(T) in **a** and **b**. In order to compare the difference between AT and GC, water molecules concentrated on O2(T) is additionally counted. O2(T) does not contribute to hydrogen bonds in a complementary AT pair. Therefore, O2(T) usually attracts solvent water molecules and the increase of water molecules due to base pair cleavages is very few. The concentration of water molecules around O2(T) is remarkable near 1.9 Å. Figure 3c shows the distributions of water molecules around O4(T). In this case, water molecules attracted to O4(T) increase as base pairs are cleaved. The concentration of water molecules is remarkable at the distance of near 1.9 Å and the density at 1.9 Å is higher than that of pure water. However, compared with the case of N1(A), high concentration of water molecules is observed around O4(T) regardless of whether the base pairs are bonded or not. Table 2 presents the number of water molecules within 2.5 Å and 3.4 Å from N1(A), O2(T), or O4(T). The standard deviations resulting from 6 trials are in parentheses. It is known that the nearest hydration shell, caused by strong hydrogen bonds, is mainly formed within 2.5 Å from base atoms [34] and that the second shell is stabilized by VDW interactions within 3.2 Å [34] or 3.4 Å [44]. Therefore, in the present study, the amount of water molecules within 2.5 Å and 3.4 Å is especially focused. As mentioned above, the water molecules attracted by N1(A) drastically increases with the base pair cleavages. In particular, within 3.4 Å, the number of 2.3 water molecules concentrate on N1(A) in **b**, which is 10 times as many as that in **a**. On the other hand, more than one water molecule usually forms hydrogen bonds with O2(T) and O4(T) within 2.5 Å. Increase of water molecules around O2(T) and O4(T) is also obtained in **b**. O2(T) and O4(T) approximately attract 3.1 and 3.3 water molecules within 3.4 Å, respectively. Compared with the double strand B–DNA, approximately twice the number of water molecules aggregates near O2(T) and O4(T). Hydration of water molecules at the dissociated sites is enhanced by base pair cleavages. It is suggested that the diffusivity of DNA fragments is influenced by hydrated water molecules. In previous reports [35, 36, 44–46], the total amount of hydrated water molecules to a nucleotide pair was evaluated as about 20 molecules. This indicates that hydration by water molecules is a long range effect and that base atoms interact weakly with water molecules over the nearest hydration shell. In addition, hydrated structures around phosphate groups on the backbones and the other base atoms were experimentally and theoretically well investigated [47–49]. However, hydrated structures around denatured base pairs and their effects on the diffusivity have not been discussed enough. In this study, the hydration effect is investigated particularly in the context of diffusivity change which is expected to be effective for the sequence separations. Figure 4 shows mean square displacements obtained from the MD computations for **a** and **b**. Each plot is summarized as the average of 6 trials. Reddy et al. [50] investigated that the displacements of B–DNA decamer were confirmed to be approximately 2.0 Å after 600 ps samplings. Compared with the previous results, our computations are reasonable. In each trial, it was confirmed that DNA fragments moved near the equilibrium conditions, although their motions were driven by collisions with water molecules. During the MD samplings, the temperature was averagely maintained at 300 K. The linearity of the plots is adjusted by the least square approximation. According to Eq. 2.2, the diffusion coefficients of **a** and **b** are calculated as 1.4×10^{-10} and 0.87×10^{-10} m^2/s, respectively. In addition, the standard deviations of **a** and **b** are 0.62×10^{-10} and 0.26×10^{-10} m^2/s,

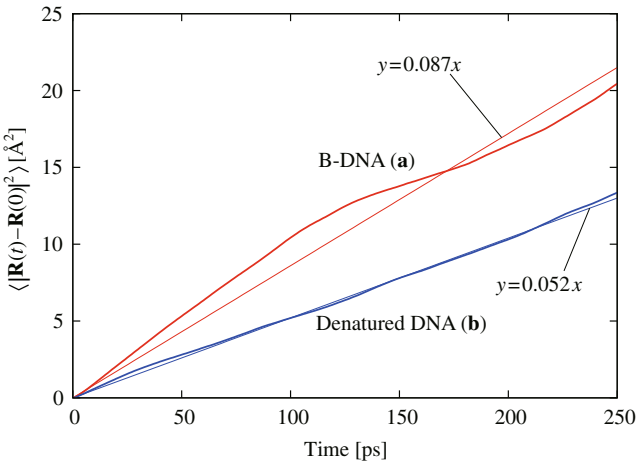

Fig. 4 Mean square displacement of B–DNA (**a**) and denatured DNA (**b**). Diffusivity reduction is observed in denatured DNA decamer due to base pair cleavages

respectively. The order of these diffusion coefficient 10^{-10} m^2/s is confirmed to be reasonable, compared with the results of 18-mer of DNA [51] and 6-mer of RNA [52]. The diffusivity of DNA decamer is more reduced in the case of **b** than that in the case of **a**.

The diffusion coefficient of Eq. 2.2 is also represented by

$$D = \frac{k_B T}{m\gamma}, \tag{3.1}$$

according to the Einstein relation. Here, the parameters of m, γ, k_B, and T are the mass of molecule, a friction coefficient, the Boltzmann constant, and temperature, respectively. In constant temperature conditions, the diffusion coefficient depends on the mass and the friction coefficient. When the diffusion coefficient is affected by the changes of mass Δm and friction coefficient $\Delta\gamma$, an updated diffusion coefficient D' is represented as follows:

$$D' = \frac{k_B T}{(m+\Delta m)(\gamma+\Delta\gamma)}. \tag{3.2}$$

Here, if $\Delta m\Delta\gamma/m\gamma$ is negligibly small, then

$$\frac{\Delta m}{m} + \frac{\Delta\gamma}{\gamma} \simeq \frac{D}{D'} - 1, \tag{3.3}$$

where Eq. 3.1 is inserted into Eq. 3.2. In the present case, the mass is changed by the hydration effect and the friction coefficient is affected by the morphology changes, although these effects cannot be separated completely in this study. Because the friction coefficient should be determined in the steady states under external force fields. Based on Eq 3.3, the difference of diffusion coefficients between **a** and **b** is analyzed. If the consideration of $\Delta m/m \gg \Delta\gamma/\gamma$ is acceptable, the mass increase is estimated as follows:

$$\frac{\Delta m}{m} = \frac{1.4\times10^{-10}}{0.87\times10^{-10}} - 1 = 0.61. \tag{3.4}$$

According to the molecular mass of **a** and **b**: 6034, the increase of mass is estimated as $\Delta m \simeq 3676$. This value corresponds to 204 water molecules that adsorb to **b**. That is, approximately 26 ($\simeq$ 204/8) water molecules contribute to the hydration of a base pair cleavage.

Under rough estimation, the increase of hydrated water molecules can be counted from the radial distribution functions. In Fig. 3, apparently two peaks are obtained within 6.0 Å in each case. The first peak near 2.0 Å is caused by the Coulomb interaction and the second peak near 4.0 Å is by the VDW interaction. Considering water molecules attracted by these interactions, the radial ditribution functions are integrated up to 5.0, 5.8, and 5.8 Å for N1(A), O2(T), and O4(T), respectively, including the minima outside the second peaks. As a result, the increase of water molecules is evaluated as 11, 6, and 6 to N1(A),

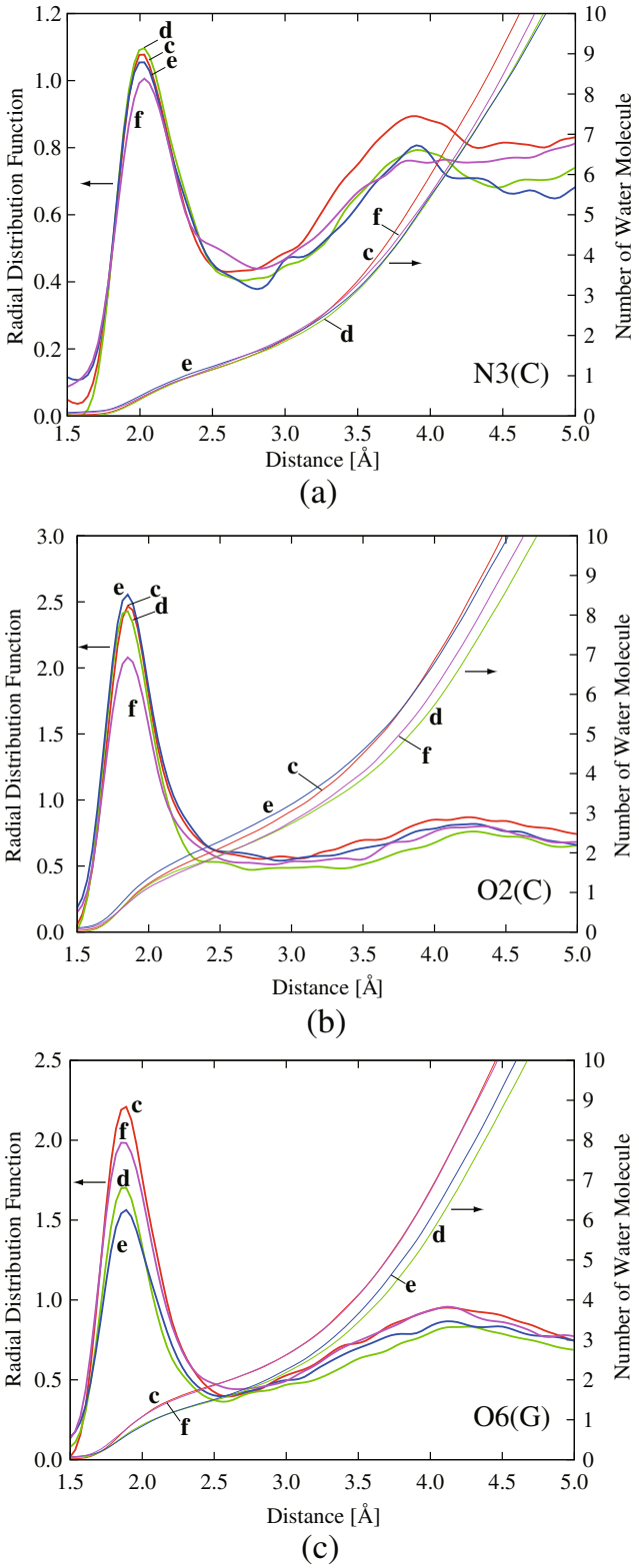

Fig. 5 Radial distribution function and number of water molecules around (**a**) N3(C), (**b**) O2(C), and (**c**) O6(G). Aggregation of water molecules near N3(C) is enhanced by melting and water molecules particularly concentrate on O2(C) and O6(G)

Table 3 Amount of water molecules within 2.5 and 3.4 Å around N3(C), O2(C), and O6(G). Standard deviations are in parentheses

	N3(C)		O2(C)		O6(G)	
	2.5 Å	3.4 Å	2.5 Å	3.4 Å	2.5 Å	3.4 Å
c	1.2 (0.2)	3.0 (0.2)	2.1 (0.3)	4.1 (0.5)	1.9 (0.2)	3.8 (0.2)
d	1.2 (0.2)	2.8 (0.4)	2.0 (0.1)	3.6 (0.4)	1.5 (0.2)	3.1 (0.4)
e	1.2 (0.0)	2.8 (0.1)	2.3 (0.1)	4.3 (0.2)	1.5 (0.3)	3.3 (0.6)
f	1.2 (0.1)	2.9 (0.2)	1.9 (0.2)	3.8 (0.3)	1.9 (0.0)	3.7 (0.2)

O2(T), and O4(T), respectively and the total increase is approximately 23. Therefore, the value of $\Delta m/m$ in Eq. 3.4 that concludes 26 hydrated water molecules can be acceptable. As mentioned above, this difference in the diffusion coefficients partly attribute to the hydration effect to the dissociated base atoms. On the other hand, it is considered that complicated conformations caused by the base pair cleavages increase the hydrodynamic radius of molecules. Collisions with solvent molecules usually increase the hydrodynamic resistance as the hydrodynamic radius increases. In the present case, the hydrodynamic radius of the denatured DNA fragment is probably larger than that of the complete double strand structure. Regardless of the ratio of the mass increase to the morphology change, the diffusivity of denatured DNA fragments is reduced according to Eq. 3.1. Consequently, it is suggested that the difference of DNA structures is possibly separated.

Characteristics of diffusivity caused by single nucleotide polymorphisms

Additional MD computations are performed for mutations of **b** in order to discuss the influence of SNPs on the diffusivity. Four types of the substitution in which A4T17, A6T15, A8T13, or A10T11 are replaced by a GC pair are prepared. Hereafter, these substitutions are referred to as **c**, **d**, **e**, and **f**, respectively. Details of these sequences are presented in Table 1. Figure 5 shows distributions of water molecules around N3(C), O2(C), and O6(G) of the substituted parts. These atoms become bare due to the base pair cleavages. In each case, water molecules tend to aggregate near 1.9 Å around O2(C) and O6(G), and near 2.0 Å around N3(C). These peak points seem to be similar to those at 1.9 Å around O2(T) and O4(T) and at 2.0 Å around N1(A) as shown in Fig. 3. Figure 5b and c show the concentrations of water molecules near 1.9 Å from O2(T) and O6(G) are higher than that of pure water. In addition, the amount of water molecules concentrated around dissociated GC pairs shows different characteristics from those around dissociated AT pairs. Table 3 presents the number of water molecules within 2.5 Å and 3.4 Å from N3(C), O2(C), and O6(G) for the same reason with the previous discussion. The amounts of water molecules within 2.5 Å around N3(C), O2(C), and O6(G) are 1.2, between 1.9 and 2.3, and between 1.5 and 1.9, respectively. VDW interactions also seem to be effective near dissociated GC pairs. Within 3.4 Å, water molecules that aggregate around N3(C), O2(C), and O6(G) are approximately 2.9, 3.9, and 3.5, respectively. Each amount is more than that of N1(A), O2(T), and O4(T) in AT pairs, which is evaluated as 2.3, 3.1, and 3.3, respectively. Water molecules tend to concentrate more densely around dissociated GC pairs than around dissociated AT pairs. Differences in hydrated structures about AT and GC were also discussed by Chalikian et al. [45] and Schneider et al. [44]. They indicate that GC tends to attract more water molecules than AT caused by hydrophilic N2(G) and hydrophobic methyl group in thymine. Those N2(G) and methyl group may affect the hydration properties of dissociated GC pairs, although details of those effects have not been clarified enough in this study. Figure 6 shows mean square displacements of **c**, **d**, **e**, and **f** in the same manner as Fig. 4. In each model, results from 6 trials show good linearity. The diffusion coefficients are evaluated as 1.5×10^{-10}, 1.3×10^{-10}, 1.1×10^{-10}, and 1.3×10^{-10} m^2/s for **c**, **d**, **e**, and **f**, respectively. Standard deviations of these diffusion coefficients are 0.58×10^{-10}, 0.43×10^{-10}, 0.43×10^{-10}, and 0.51×10^{-10} m^2/s, respectively. On the other hand, the diffusion coefficient of b and its standard deviation are calculated as 0.87×10^{-10} m^2/s and 0.26×10^{-10} m^2/s,

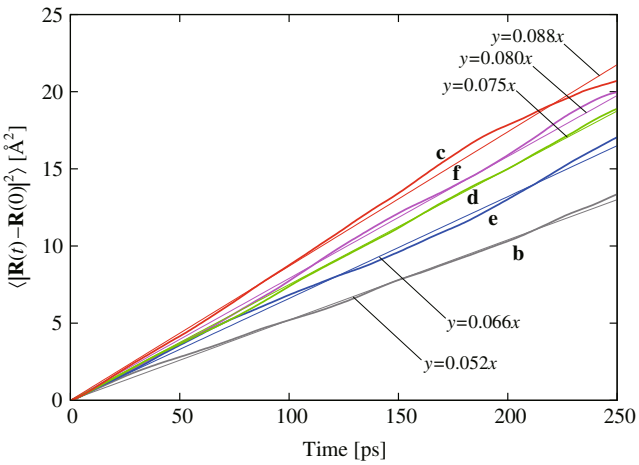

Fig. 6 Mean square displacement of the case **b** and its single nucleotide polymorphisms: **c**, **d**, **e**, and **f**. Diffusivity of these polymorphisms appears to be larger than that of **b**

respectively. The value of **b** is evaluated smaller than those of the other substitutions. The increase of diffusion coefficients is obtained by substituting AT with GC in a part of the sequences. Substitutions of GC for AT are considered to be sensitive to their diffusivity, although differences between **c**, **d**, **e**, and **f** are not clarified in detail. According to the previous discussion based on Eqs. 3.1–3.4, the difference between **b** and **c**–**f** seems to be influenced by their differences of morphology as well as the mass increase by hydrated water molecules that adsorbed on the dissociated base molecules. The influence of friction coefficient on the diffusion coefficient should be clarified in our future study, investigating steady flows of DNA fragments under external electric fields. As a result, it is implied that single nucleotide substitutions influence the diffusivity changes. In this case, water molecules attracted to N1(A) and N3(C) tend to increase with the base pair cleavages and cause it to reduce the diffusivity. Additionally, broken symmetries in the sequences of **c**, **d**, **e**, and **f**, compared with **a** and **b**, seem to influence the difference of diffusion coefficients. It is suggested that denatured DNA fragments are dragged by aggregated water molecules and that differences in the single nucleotide polymorphisms contribute to change the diffusivity. These results appear to contradict the discussion about mass increases that cause the reduction of diffusivity [13]. On the other hand, our results indicate that the motions of DNA fragments are more activated by water molecules as the dissociated base molecules are increasingly hydrated because the dissociated base pairs turn to be hydrophilic and attract more solvent water molecules.

Conclusion

In the present study, the diffusivity of 10 bp DNA fragments in water solvent has been discussed focusing on the molecular structures and single nucleotide polymorphisms. Results from our numerical analyses are summarized as follows. (i) It was clarified that base pair cleavages changed the diffusivity of DNA fragments. Differences in the molecular structures of DNAs clearly appeared in the difference of diffusion coefficients. In particular, the number of hydrated water molecules increased around N1(A) in 5'- dCGTATATATA-3' as AT base pairs were dissociated and the decrease of diffusion coefficients turned out to be remarkable due to the base pair cleavages. The reduction of diffusion coefficients was mainly affected by the mass increase of hydrated water molecules. This conclusion was confirmed by the Einstein relation and the radial distribution functions. (ii) Substitutions of the base sequence were also effective to change the diffusivity. It was suggested that the diffusion coefficients of DNA fragments tended to be increased by substituting AT with GC. There was a difference in the amount of water molecules that formed hydrogen bonds with dissociated AT or GC base pairs. N3(C), O2(C), and O6(G) formed hydrated shell with approximately 2.9, 3.9, and 3.5 water molecules within 3.4 Å, respectively, although such a high concentration was not observed in dissociated AT base pairs. (iii) It is indicated that dissociated base pairs that enhance making hydrogen bonds with surroundings are effective in electrophoretic analyses such as DGGE, TGGE, and CE, and that observations of SNPs are partly caused by the different characteristics in the diffusivity of denatured DNAs.

References

1. Myers RM, Fischer SG, Lerman LS, Maniatis T (1985) Nearly all single base substitutions in DNA fragments joined to a GC-clamp can be detected by denaturing gradient gel electrophoresis. Nucleic Acids Res 13:3131–3145
2. Steighner RJ, Tully LA, Karjala JD, Coble MD, Holland MM (1999) Comparative identity and homogeneity testing of the mtDNA HV1 region using denaturing gradient gel electrophoresis. J Forensic Sci 44:1186–1198
3. Buch JS, Kimball C, Rosenberger F, Highsmith WE Jr, DeVoe DL, Lee CS (2004) DNA mutation detection in a polymer microfluidic network using temperature gradient gel electrophoresis. Anal Chem 76:874–881
4. Danko P, Kozák A, Podhradský D, Víglaský V (2005) Analysis of DNA intercalating drugs by TGGE. J Biochem Biophys Methods 65:89–95
5. Yasuda M, Shiaris MP (2005) Differentiation of bacterial strains by thermal gradient gel electrophoresis using non-GC-clamped PCR primers for the 16S–23S rDNA intergenic spacer region. FEMS Microbiology Lett 243:235–242
6. Nataraj AJ, Olivos-Glander I, Kusukawa N, Highsmith WE Jr (1999) Single-strand conformation polymorphism and heteroduplex analysis for gel-based mutation detection. Electrophoresis 20:1177–1185
7. Nakatani K (2004) Chemistry challenges in SNP typing. Chembiochem 5:1623–1633
8. Peck K, Wung S-L, Chang G-S, Yen JJ, Hsieh Y-Z (1997) Restriction mapping of genes by capillary electrophoresis with laser-induced fluorescence detection. Anal Chem 69:1380–1384
9. Mansfield ES, Robertson JM, Vainer M, Isenberg AR, Fraziel RR, Ferguson K, Chow S, Harris DW, Barker DL, Gill PD, Budowle B, McCord BR (1998) Analysis of multiplexed short tandem repeat (STR) systems using capillary array electrophoresis. Electrophoresis 19:101–107
10. Schwinefus JJ, Morris MD (1999) Periodicity of λ DNA motions during field inversion electrophoresis in dilute hydroxyethyl cellulose visualized by high-speed video fluorescence microscopy. Macromol 32:3678–3684
11. Klepárník K, Boček P (2007) DNA diagnostics by capillary electrophoresis. Chem Rev 107:5279–5317
12. Kaji N, Tezuka Y, Takamura Y, Ueda M, Nishimoto T, Nakanishi H, Horiike Y, Baba Y (2004) Separation of long DNA molecules by quartz nanopillar chips under a direct current electric field. Anal Chem 76:15–22
13. Balducci A, Mao P, Han J, Doyle P (2006) Double-stranded DNA diffusion in slitlike nanochannels. Macromol 39:6273–6281
14. Li B, Fang X, Luo H, Seo Y-S, Petersen E, Ji Y, Rafailovich M, Sokolov J, Gersappe D, Chu B (2006) Separation of DNA with

different configurations on flat and nanopatterned surfaces. Anal Chem 78:4743–4751
15. Tsutsui M, Taniguchi M, Kawai T (2009) Transverse field effects on DNA-sized particle dynamics. Nano Lett 9:1659–1662
16. Salieb-Beugelaar GB, Teapal J, van Nieuwkasteele J, Wijnperlé D, Tegenfeldt JO, Lisdat F, van den Berg A, Eijkel JCT (2008) Field-dependent DNA mobility in 20 nm high nanoslits. Nano Lett pp. 1785–1790
17. Taniguchi M, Kawai T (2006) DNA electronics. Physica E 33:1–12
18. Nagahiro S, Kawano S, Kotera H (2007) Separation of long DNA chains using a nonuniform electric field: a numerical study. Phys Rev E 75:011902-1–011902-5
19. Zhao X, Payne CM, Cummings PT (2008) Controlled translocation of DNA segments through nanoelectrode gaps from molecular dynamics. J Phys Chem Lett C 112:8–12
20. Zwolak M, Ventra MD (2008) Colloquium: physical approaches to DNA sequencing and detection. Rev Mod Phys 80:141–165
21. Doi K, Yonebayashi T, Kawano S (2010) Perturbation theory analysis for electronic response of DNA base pairs. J Mol Struct: THEOCHEM 939:97–105
22. Kawano S (1998) Molecular dynamics of rupture phenomena in a liquid thread. Phys Rev E 58:4468–4472
23. Hanasaki I, Haga T, Kawano S (2008) The antigen-antibody unbinding process through steered molecular dynamics of a complex of an Fv fragment and lysozyme. J Phys Condens Matter 20:255238-1–255238-10
24. Hanasaki I, Shintaku H, Matsunami S, Kawano S (2009) Structural and tensile properties of self-assembled DNA network on mica surface. Comput Model Eng Sci 46:191–207
25. Drew HR, Dickerson RE (1981) Structure of a B–DNA dodecamer III. Geometry of hydration J Mol Biol 151:535–556
26. Seibel GL, Singh UC, Kollman PA (1985) A molecular dynamics simulation of doublehelical B–DNA including counterions and water. Proc Nat Acad Sci USA 82:6537–6540
27. Kurinov IV, Krupyanskii YF, Panchenko AR, Suzdalev IP, Uporov IV, Shanitan KV, Rubin AB, Goldanskii VI (1990) Intramolecular dynamics of hydrated DNA studied by rayleigh scattering of m¨ossbauer radiation (RSMR). Hyperfine Interact 58:2355–2358
28. Auffinger P, Westhof E (2000) Water and ion binding around RNA and DNA (C, G) oligomers. J Mol Biol 300:1113–1131
29. Chatake T, Tanaka I, Umino H, Arai S, Niimura N (2005) The hydration structure of a Z–DNA hexameric duplex determined by a neutron diffraction technique. Acta Crystallogr D61:1088–1098
30. Shi X, Macgregor RB Jr (2007) Volume and hydration changes of dna–ligand interactions. Biol Chem 125:471–482
31. Kistner C, André A, Fischer T, Thoma A, Janke C, Bartels A, Gisler T, Maret G, Dekorsyb T (2007) Hydration dynamics of oriented DNA films investigated by time-domain terahertz spectroscopy. Appl Phys Lett 90:233902-1–233902-3
32. Toporowski JW, Reddy SY, Bruice TC (2007) An investigation of the ionic and solvation patterns of dsDNG versus dsDNA by use of molecular dynamics simulations. Biol Chem 126:132–139
33. Doi K, Haga T, Shintaku H, Kawano S (2010) Development of coarse graining DNA models for single nucleotide resolution analysis. Phil Trans R Soc A 368:2615–2628
34. Chuprina VP, Heinemann U, Nurislamov AA, Zielenkiewicz P, Dickerson RE, Saenger W (1991) Molecular dynamics simulation of the hydration shell of a B-DNA decamer reveals two main types of minor-groove hydration depending on groove width. Proc Natl Acad Sci USA 88:593–597
35. Brovchenko I, Krukau A, Oleinikova A, Mazur AK (2007) Water clustering and percolation in low hydration DNA shells. J Phys Chem B 111:3258–3266
36. Mazur AK (2008) The electrostatic origin of low-hydration polymorphism in DNA. Chemphyschem 9:2691–2694
37. Lewin B (2008) Genes IX. Jones and Bartlett, Sudbury, p 13
38. Shimizu N, Kawano S, Tachikawa M (2005) Electron correlated and density functional studies on hydrogen-bonded proton transfer in adenine–thymine base pair of DNA. J Mol Struct 735–736: 243–248
39. Mark P, Nilsson L (2001) Structure and dynamics of the TIP3P, SPC, and SPC/E water models at 298 k. J Phys Chem A 105:9954–9960
40. Ryckaert J-P, Ciccotti G, Berendsen HJC (1977) Numerical integration of the cartesian equations of motion of a system with constraints: molecular dynamics of n-Alkanes. J Comput Phys 23:327–341
41. Ponder JW, Case DA (2003) Force fields for protein simulations. Adv Protein Chem 66:27–85
42. Case DA, Darden TA, Cheatham TE III, Simmerling CL, Wang J, Duke RE, Luo R, Crowley M, Walker RC, Zhang W, Merz KM, Wang B, Hayik S, Roitberg A, Seabra G, Kolossváry I, Wong KF, Paesani F, Vanicek J, Wu X, Brozell SR, Steinbrecher T, Gohlke H, Yang L, Tan C, Mongan J, Hornak V, Cui G, Mathews DH, Seetin MG, Sagui C, Babin V, Kollman PA (2008) computer code Amber 10. University of California, San Francisco
43. Allen MP, Tildesley DJ (1989) Computer simulation of liquids. Oxford University Press, Oxford, p 60
44. Schneider B, Berman HM (1995) Hydration of the DNA bases is local. Biophys J 69:2661–2669
45. Chalikian TV, Sarvazyan AP, Plum GE, Breslauer KJ (1994) Influence of base composition, base sequence, and duplex structure on DNA hydration: apparent molar volumes and apparent molar adiabatic compressibilities of synthetic and natural dna duplexes at 25°C. Biochemistry 33:2394–2401
46. Pal SK, Zhao L, Zewail AH (2003) Water at DNA surfaces: ultrafast dynamics in minor groove recognition. Proc Natl Acad Sci USA 100:8113–8118
47. Tsukamoto T, Ishikawa Y, Natsume T, Dedachi K, Kurita N (2007) A combined molecular dynamics/density-functional theoretical study on the structure and electronic properties of hydrating water molecules in the minor groove of decameric DNA duplex. Chem Phys Lett 441:136–142
48. Komura I, Ishikawa Y, Tsukamoto T, Natsume T, Kurita N (2008) Density-functional calculations of hydrated structures and electronic properties for G–C and A–T base pairs. J Mol Struct: THEOCHEM 862:122–129
49. Berashevich J, Chakraborty T (2008) Water induced weakly bound electrons in DNA. J Chem Phys 128:235101-1–235101-6
50. Reddy SY, Leclerc F, Karplus M (2003) DNA polymorphism: a comparison of force fields for nucleic acids. Biophys J 84:1421–1449
51. Nkodo AE, Garnier JM, Tinland B, Ren H, Desruisseaux C, McCormick LC, Drouin G, Slater GW (2001) Diffusion coefficient of DNA molecules during free solution electrophoresis. Electrophoresis 22:2424–2432
52. Yeh I-C, Hummer G (2004) Diffusion and electrophoretic mobility of single-stranded RNA from molecular dynamics simulations. Biophys J 86:681–689